The Interferometer, Fringe Frequencies, Solving for Baseline Values, and the Diameter of the Sun

Author: Sam Johnson

April 4, 2017

Abstract

This lab was focused on understanding the many uses of the interferometer. It was used to record fringe data from both a point source Cas A and extended sources, the Sun and Moon. The main objectives of this lab were to determine the baseline of the interferometer with high precision as well as to determine the angular diameter of the Sun and Moon. We were unable to determine the diameter of the Moon, but the Sun's diameter was calculated to be roughly .47 degrees, fairly close to the known .50 degrees.

1. Introduction

Interferometers are very useful instruments in astronomy. Superimposed waves from sources in space naturally create interference patterns as they construct and destruct. Interferometry takes requires using two telescopes which allows researchers to extrapolate more specific information than a singular telescope could. In this lab we explore the usefulness of such a set up by analyzing the unique fringe patterns generated by interferometers, and using this analysis to make further conclusions regarding the emitting bodies which we measure.

2. Interferometer

2.1 Theory

Interferometers utilize multiple telescopes. When both telescopes are pointed at the same source, there is a slight time difference between the time one dish receives a signal compared to the other, and this difference is based geometrically on the angle of the source and the distance between the two dishes. This geometric time difference is known as τ_g. However, this is not the only difference that will affect the data as it is recorded. Another delay, τ_{cable}, comes from any difference in the distance between the two dishes and the sampler. Thus, the total difference is

$$\tau_{total} = \tau_g(ha) + \tau_{cable} \tag{1}$$

The time difference τg is a function of hour angle. This is because the delay depends on the position of the source in the sky, and sources change relative positions in the sky as Earth rotates. At higher angles, the time difference is the least. There is no time difference if the object being observed is directly overhead of the two dishes. Logically, the time difference is greatest when objects are at lower levels, as the distance between the two dishes has more impact on the data. As such, τg is accurately represented as function of hour angle.

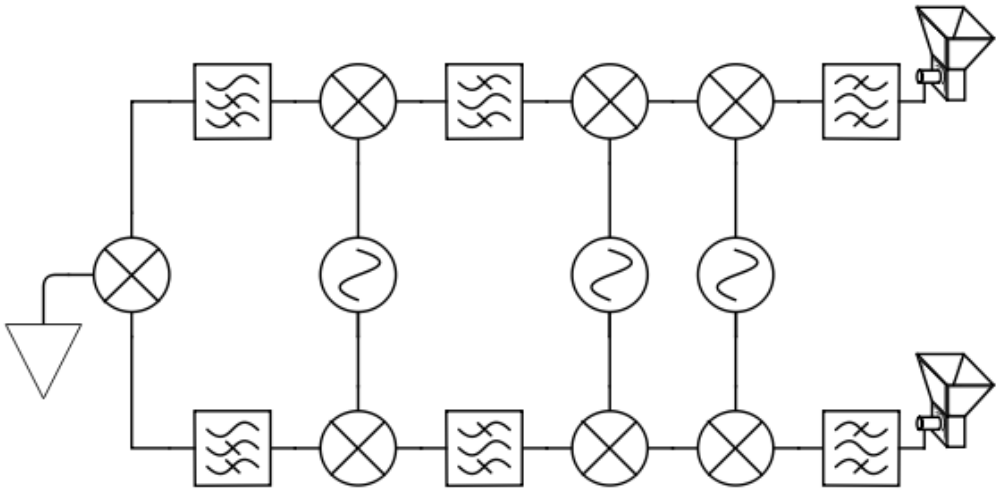

Figure 1: Diagram of the interferometer system.

The signals received by the two dishes are combined to form a multiplying interferometer. This two signals, E_1 and E_2, and sent through a mixer and multiplied, and their product is shown below:

$$(E_1 + E_2)^2 = E_1^2 + E_2^2 + 2E_1E_2 \tag{2}$$

The most relevant data is the product E_1E_2 of the signals, so the self-products of the signals E_1^2 and E_2^2 are subtracted to isolate this product for analysis.

An important factor in the signal which is recorded is the baseline between the two dishes, B. This distance is a vector, which can be split into two components based on direction. B_{ew} represents the component of the baseline that aligns in the east-west direction, and B_{ns} represents the other component which aligns in the north-south west direction. These two components have a reliance on many factors, and their relationship is shown below.

$$\tau_{g,ew}(h_a) = [\frac{B_{ew}}{c}\cos\delta]\sin h_a \tag{3}$$

$$\tau_{g,ns}(h_a) = [\frac{B_{ns}}{c}\sin L\cos\delta]\cos h_a - [\frac{B_{ns}}{c}\cos L\sin\delta] \tag{4}$$

In this expression, h_s is the hour angle, L is the latitude on Earth at which the telescopes are located, and δ is the declination of the source in the sky.

The second term in equation 4 is not dependent on the hour angle, so it can be moved to the non-time dependent component in the cable delay. The two hour angle dependent components can be combined into one geometrically determined delay, τ_g', and the remaining components form τ_c' as shown in equations 5 and 6 below.

$$\tau_c' = \tau_c - [\frac{B_{ns}}{c}\cos L\sin\delta] \tag{5}$$

$$\tau_g'(h_s) = [\frac{B_{ew}}{c}\cos\delta]\sinh_s + [\frac{B_{ns}}{c}\sin L\cos\delta]\cos h_s \tag{6}$$

2.1 Fringe

Factoring in the effect of this time delay creates the fringe. The equations that represent the voltages of the two sources are

$$E_1(t) = \cos(2\pi\nu t) \tag{7}$$

$$E_2(t) = \cos(2\pi\nu[t + \tau_{tot}]) \tag{8}$$

Upon multiplying the two as in equation 2, we can use various trigonometric identities to change the expression to something vastly more useful. First it can be converted from multiplied sinusoids into a single sinusoid that features a product of two variables inside it. Another well known identity allows us to convert the singular cosine function to the following equation, :

$$F(h_s) = \cos(2\pi\nu\tau_c)\cos(2\pi\nu\tau_g') - \sin(2\pi\nu\tau_c)\sin(2\pi\nu\tau_g') \tag{9}$$

This equation is most useful because it is in terms of one variable, after the assumption that the right ascension is well known enough to determine h_s which allows it to be included in the τ_g term. Since $\cos(2\pi\nu\tau_c)$ and $\sin(2\pi\nu\tau_c)$ are constants, they can be replaced with arbitrary A and B and solved with least squares. This yields the final fringe equation:

$$F(h_s) = A\cos(2\pi\nu\tau_g') + B\sin(2\pi\nu\tau_g') \tag{10}$$

3. Data

3.1 Cas A

We chose to observe the object Cas A as our point source. The object is located with right ascension 23^h23^m24s and a declination of $+58°48.9'$. Using the rotation matrix we created for the previous lab, we were able to convert these galactic coordinates to azimuth and altitude coordinates for use here on Earth. After doing so, we had to determine when Cas A rose and set over the horizon. This was done by calculating at what time the altitude of Cas A was zero, and adjusting to the values to see if its altitude was increasing or decreasing. We determined it rose at about 6am, and around 6pm it would set behind Evans so we could no longer take data. All in all, we recorded a good 12 hours of data for use. After collecting the data, some basic analysis was done, including a Fourier transform to frequency space and computing a power spectrum.

3.2 The Sun

The Sun, unlike Cas A, is not a point source as it subtends a visible angle in the sky. As an extended source, the Sun's fringe frequency and amplitude changes with time. Likewise, its declination is not constant since it is close enough to Earth to have noticeable changes in relative motion. Our procedure for capturing a days' worth of data for the Sun was essentially identical to that of our procedure with Cas A. We used the `isun` procedure and followed the sun for 12 hours. Below are the raw voltage data, the transformed voltage spectrum, and the power spectrum.

The fringe data shows very clear patterns as the sun nears the horizon, which is to be expected since the the phase delay is greatest when objects are near the horizon. In regards to the power spectrum, there are multiple clear peaks

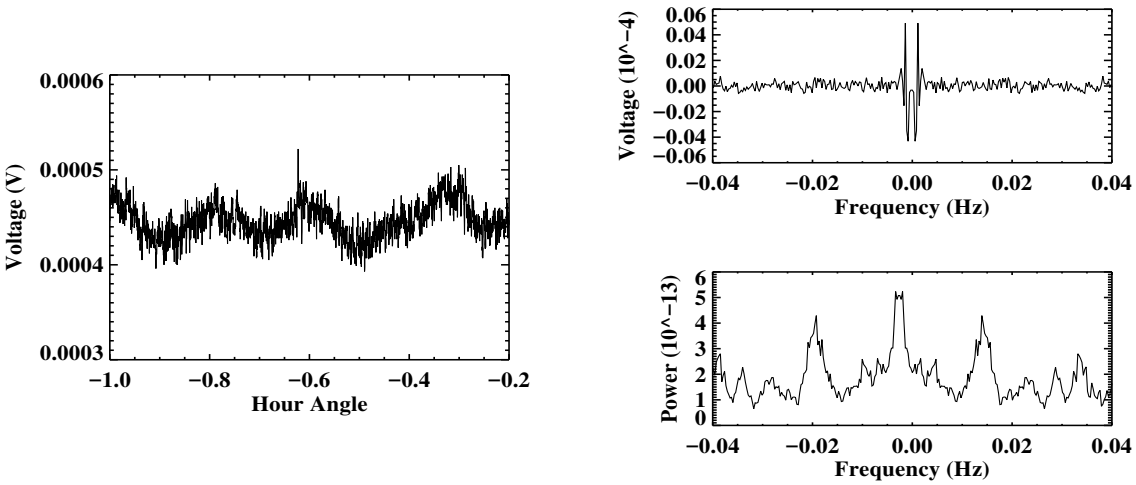

Figure 2: Cas A raw voltage data, voltage spectrum, and power spectrum.

v

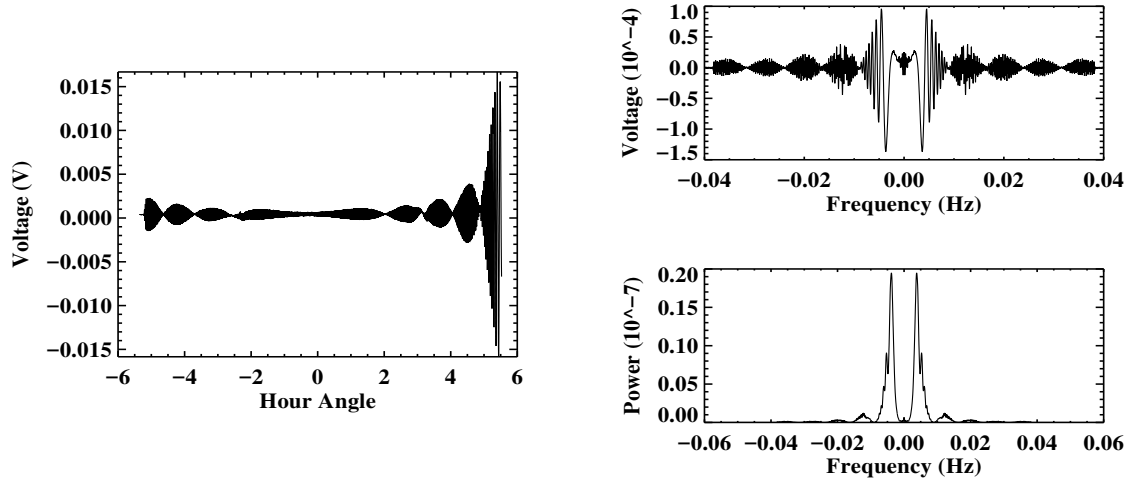

Figure 3: Raw voltage data, voltage spectrum, and power spectrum for the Sun.

3.3 The Moon

Observation of the moon unsurprisingly occurred at night while the sun was down to ensure the most direct unobstructed signal could be obtained. The `imoon` procedure allowed us to follow the moon and account for its even greater relative motion since it orbits us. Below are the raw voltage data, the transformed voltage spectrum, and the power spectrum.

Unfortunately, our data for the Moon was very poor. The raw data didn't oscillate about zero and there were no indications of sinusoidal fringe patterns like the Sun. In an attempt to correct this, I tried smoothing the raw data and then subtracting that from the original data to center it about 0. This worked in centering it, but made the data pretty unusable. As a result, in the later sections asking for the diameters of the Sun and Moon, only the Sun is covered due to difficulty getting a result of any meaning out of the Moon data.

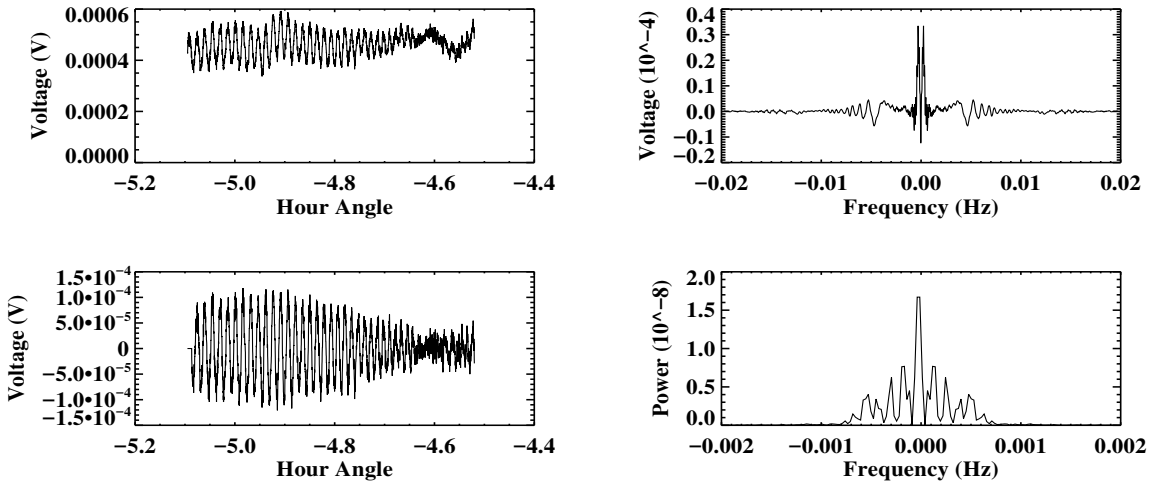

Figure 4: The voltage spectrum and power spectrum of the Sun.

4. Local Fringe Frequency

The final result for the fringe amplitude is a function of h_s as seen below:

$$F(h_s) = A\cos(2\pi\nu\tau_g') + B\sin(2\pi\nu\tau_g') \tag{11}$$

However, upon closer inspection and realization that the h_s term lies inside τ_g', it becomes clear that the function of h_s is not linear but sinusoidal since it lies in both a *sin* and *cos*. This frequency at which they oscillate is know as the local fringe frequency, f_f.

$$\sin(h_s) = \sin(h_{s,0}) + \Delta h_s \frac{d\sin(h_s)}{dh}|_{h_s} \sin(h_{s,0}) + \Delta h_s \cos(h_{s,0}) \tag{12}$$

We take the Taylor expansion of $\sin h_s$ about a certain hour angle $h_{s,0}$, and the second term provides the behavior of this function about this hour angle. The fringe amplitude $F(h_s)$ changes with $f_f \Delta h_s$, with f_f shown below.

$$f_f = [\frac{B_{ew}}{\lambda}\cos\delta]\cos h_{s,0} - [\frac{B_{ns}}{\lambda}\sin L\cos\delta]\sin h_{s,0} \tag{13}$$

5. Determining $B\cos\delta$

5.1 One Dimension

Due to the orientation of our interferometer set up, the baseline is almost entirely east-west oriented. As such for a simple sanity check we can approximate $B_{ns} = 0$ and proceed with a

simple, one dimension brute force approach to a least square fit. This was done by trying many different values for Q_{ew} over a range, and then finding the minimum. The results can be seen below. The number of Q_{ew} samples was 250, and the baseline was approximated at 19.81 m after locating the minimum residual value.

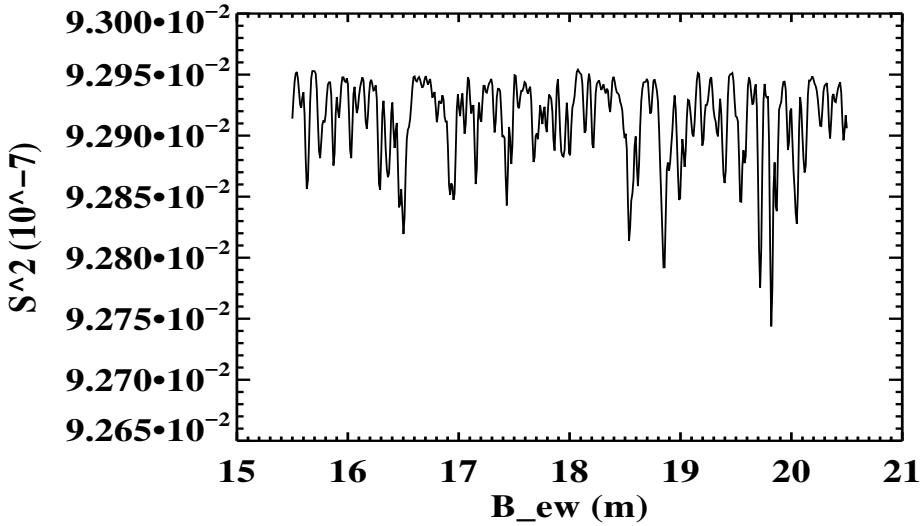

Figure 5: Square residuals for one dimensional brute force analysis.

5.2 Two Dimensions

The two dimensional approach to least squares brute force method is a bit more involved than the one dimensional method. The equations for the fringe amplitude and $\nu\tau_g'$ are below

$$F(h_s) = A\cos(2\pi\nu\tau_g') + B\sin(2\pi\nu\tau_g') \tag{14}$$

$$\nu\tau_g'(B_{ew}, B_{ns}, \delta, h_s) = [\frac{B_{ew}}{\lambda}\cos\delta]\sin h_s + [\frac{B_{ns}}{\lambda}\sin L\cos\delta]\cos h_s \tag{15}$$

In order to fit for A and B, we start by taking a set of guess values for $Q_{ew} = \left[\frac{B_{ew}}{\lambda}\cos\delta\right]$ and $Q_{ns} = \left[\frac{B_{ns}}{\lambda}\sin L\cos\delta\right]$. For each set of values of Q_{ew} and Q_{ns}, we take the least squares fit of the fringe amplitude, and obtain A and B. This gives us a set of fringe amplitudes that we may compare to our data. The calculated values are below.

$$\begin{aligned} A &= 1.302 \cdot 10^{-07} \\ B &= 6.116 \cdot 10^{-08} \end{aligned} \tag{16}$$

5.1 Uncertainties

We may compare our predicted fringe amplitude to our data and obtain the deviation from our fit. The values for Q_{ew} and Q_{ns} for which this total deviation is smallest, i.e. the residual sum of squares RSS, are our best fit values for Q_{ew} and Q_{ns}. Below we have plotted a plot of our

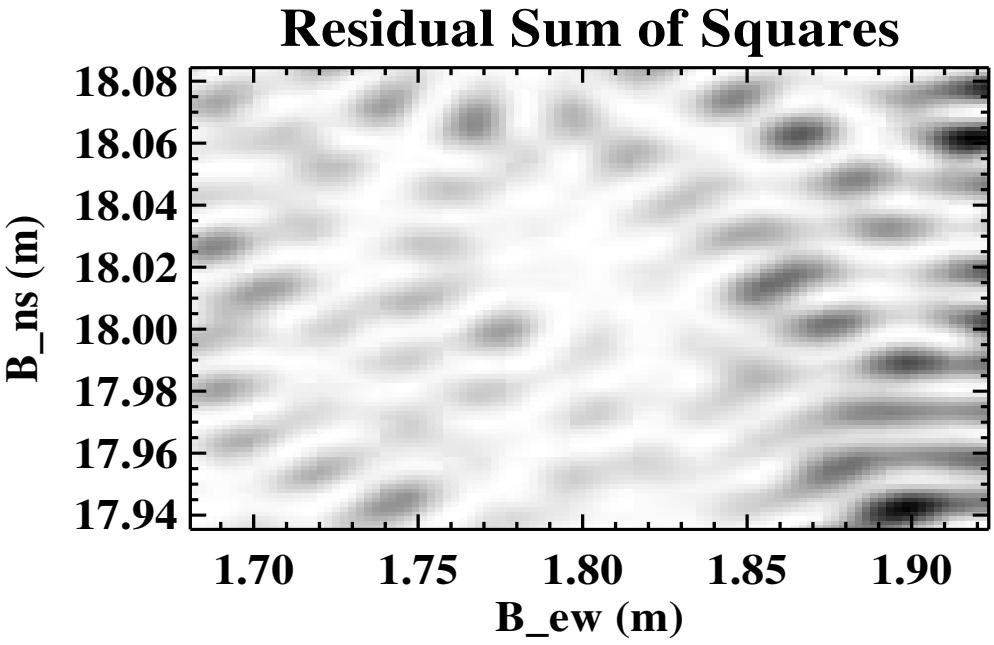

Figure 6: Residual sum of squares

sum of square residuals around the global minimum. The initial calculations were performed on Q_{ew} and Q_{ns} to obtain the global minimum. We then converted these Q values to their respective baseline values, using the following equations:

$$\begin{aligned} B_{ew} &= \frac{Q_{ew}\lambda}{\cos\delta} \\ B_{ns} &= \frac{Q_{ns}\lambda}{\sin L\cos\delta} \end{aligned} \tag{17}$$

Here, $\delta = 22.024321$ and $\lambda = \frac{c}{9.9GHz}$, where c is the speed of light in a vacuum. We obtain the values $B_{ew} = 15.10m$ and $B_{ns} = 1.59m$.
We then proceeded to find the uncertainty of our best fit values. In order to derive the uncertainties for our best-fit guess values, we solve for the curvature matrix α. This process required quite a few steps, for brevity the results are below:

$$\alpha = \begin{bmatrix} 1.426 \cdot 10^{-05} & 7.652 \cdot 10^{-06} \\ 7.652 \cdot 10^{-06} & 1.716 \cdot 10^{-05} \end{bmatrix} \tag{18}$$

In order to get the uncertainties for best-fit values for Q_{ns} and Q_{ew}, we take the inverse of our curvature matrix in order to retrieve our covariance matrix $[\alpha]^{-1}$.

$$[\alpha]^{-1} = \begin{bmatrix} 92218 & -41121 \\ -41121 & 76614 \end{bmatrix} \tag{19}$$

Using these matrices we can find the uncertainties in Q, which when converted to baseline values yield:

$$\begin{aligned} \Delta B_{ns} &= 0.145m \\ \Delta B_{ew} &= 0.107m \end{aligned} \tag{20}$$

6. Determining the Diameter of the Sun

As the sun/moon moves across the sky while the Earth rotates, they move through a fringe pattern in order to produce a fringe response as a function of time $R(h_s)$. So far, we have been working with a point source, so we have been able to take $R(h_s) = F(h_s)$ from equation **??**. The sun and moon are both extended sources, so it is important to obtain our fringe response by integrating over the source intensity. Ultimately, the interferometer response, $R(hs)$, can be expressed as so:

$$R(h_s) = \underbrace{F(h_s)}_{Point-source\ Fringe} \times \underbrace{\int I(\Delta h)\cos(2\pi f_f \Delta h)\ d\Delta h}_{Fringe\ Modulator} \tag{21}$$

We can utilize this modulating function to our own advantage. In particular, we can use it to modulate a uniformly bright disk and calculate the angular diameter of it. A uniformly bright disk with radius R is mathematically represented as:

$$I(\Delta h) = \frac{(R^2 - \Delta h^2)^{1/2}}{R} \tag{22}$$

We can use this as the point source fringe and integrating. However, instead of straining over such a complex integral, we choose to take a more rigorous numerical approach , approximating the integral as:

$$MF_{theory} \approx \delta h \sum_{n=-N}^{n=+N} \left[1 - \left(\frac{n}{N}\right)^2\right]^{1/2} \cos\left(\frac{2\pi f_f R n}{N}\right) \tag{23}$$

Using this summation, I summed over a thousand values of n. My approach toward finding the correct radius was first plotting the raw fringe data from the Sun against hour angle. Next, I created a f_f based on the data from the Sun structure. I ran this through the MF_{theory} sum and arrived at a cosine function with the only remaining variable being R. I overplotted the curve this cosine function produced on the solar fringe. From there, I simply tweaked the R value until the zeros of the cosine function aligned with those of the fringe amplitudes. The value of R I that had the best fit with the fringe data was .233°, which, when doubled, gives an angular diameter of .466°. This is fairly close to the known result of about .50°. The plot showing the overlap of the MF_{theory} with $R = .233$ and the solar fringe data is shown below.

7. Code

All of the following files can be found under the directory samhjohnson/Dekstop/LAB3.

`cas_a.pro`

Analyzes the Cas A data and creates plots of the raw data as well as the voltage and power spectra.

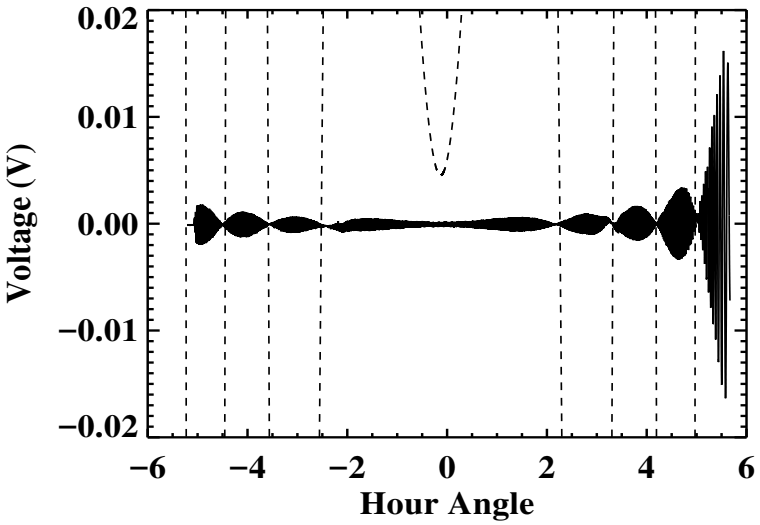

Figure 7: Raw sun data plotted against hour angle with the best fit MF overplotted.

`sun_p.pro`

Analyzes the Sun data and creates plots of the raw data as well as the voltage and power spectra.

`sun_r.pro`

Generates a modulating function and plots its over the raw sun data to create a best fit for the Sun's radius.

`moon_r.pro`

Analyzes the Moon data and creates plots of the raw data as well as the voltage and power spectra.

`baseline.pro`

Creates three procedures: oned, q, and uncertainty. Oned does the one dimensional residuals, q does the two dimensions residuals, and uncertainty calculates the uncertainties.